



## Effects of residual stresses on interlaminar radial strength of Glass-Epoxy L-bend composite laminates

M. A. Umarfarooq

Research Centre, Department of Mechanical Engineering, SDM College of Engineering & Technology, Dharwad, Visvesvaraya Technological University, Karnataka, India.

Center for Material Science, School of Mechanical Engineering, KLE Technological University, Hubballi, Karnataka, India.

[umarfarooq.ma@gmail.com](mailto:umarfarooq.ma@gmail.com)

P. S. Shivakumar Gouda\*

Research Centre, Department of Mechanical Engineering, SDM College of Engineering & Technology, Dharwad, Visvesvaraya Technological University, Karnataka, India.

[ursshivu@gmail.com](mailto:ursshivu@gmail.com)

K. N. Bharath

Department of Mechanical Engineering, GM Institute of Technology, Davangere, Visvesvaraya Technological University, Karnataka, India.

[bharathkn@gmit.ac.in](mailto:bharathkn@gmit.ac.in)

G. B. Veereshkumar

Department of Mechanical Engineering, National Institute of Technology, Tadepalligudem, Andhra Pradesh, India  
[veeru232@gmail.com](mailto:veeru232@gmail.com)

N. R. Banapurmath

Centre for Material Science, School of Mechanical Engineering, KLE Technological University, Hubballi, Karnataka, India  
[nrbanapurmath@gmail.com](mailto:nrbanapurmath@gmail.com)

Abhilash Edacherian

Department of Mechanical Engineering, College of Engineering, King Khalid University, Saudi Arabia  
[edalheriad@kku.edu.sa](mailto:edalheriad@kku.edu.sa)

**ABSTRACT.** The built-in heterogeneity of the composite laminates has been exploited to tailor the stiffness and strength requirements of modern structures to meet the specific functional demands. However, the non-homogeneity in these composites is the root cause for most of their failures.

OPEN ACCESS

Citation: Umarfarooq, M. A., Shivakumar Gouda P. S., Bharath, K. N., Veereshkumar,



One of the undesirable consequences of the inherited heterogeneity is the development of cure-induced stresses during composite manufacturing. This work aims to investigate the influence of process-induced stresses on interlaminar radial strength in curved composite laminates. Glass-Epoxy (GE) L-bend laminates of two different thicknesses are prepared by hand lamination technique using V-shaped tooling and cured under room temperature. The state of residual stresses in GE laminates is varied by post-curing these laminates at different temperatures. Curved bending strength (CBS) and corresponding interlaminar radial stress for delamination of L-bend laminates are evaluated experimentally using four points bending test. The residual stress profile in each GE laminate is experimentally characterized by employing the Slitting method. The results indicate that the residual stresses have a negligible effect on the critical stress for initial delamination in GE laminates, but the critical stress for delamination was found to be independent of the laminate thickness and increased with higher curing temperatures. The delaminated surfaces of L-bend laminates are studied using a scanning electronic microscope (SEM). The enhancement in the critical stress due to post-curing can be attributed to the improved fiber-matrix interfacial bonding with higher curing temperature.

**KEYWORDS.** L-bend composites, Residual stresses, Slitting method, Interlaminar radial stress.

G. B., Banapurmath, N. R., Edacherian, A., Effects of residual stresses on interlaminar radial strength of Glass-Epoxy L-bend composite laminates, *Frattura ed Integrità Strutturale*, 61 (2022) 140-153.

**Received:** 22.12.2021

**Accepted:** 07.04.2022

**Online first:** 29.04.2022

**Published:** 01.07.2022

Copyright: © 2022 This is an open access article under the terms of the CC-BY 4.0, which permits unrestricted use, distribution, and reproduction in any medium, provided the original author and source are credited.

## INTRODUCTION

Laminates of fiber reinforced polymer (FRP) composites with the advantages of manufacturability, high specific strength and stiffness satisfies the requirements of higher toughness for material selection and have found applications in aircraft, marine and civil structures. Curved laminates are a very common structural component in aircraft structures. These components are susceptible to failure by delamination across their thickness due to lack of reinforcement, specifically in a curved region that acts as a stress riser. It is crucial to understand the failure mechanism and the stress distribution across the curved laminates under bending load. The process-induced stresses may remain within the structures even after the manufacturing. These stresses are induced in the composites mainly due to a mismatch of thermal expansion coefficient within the matrix and fibers. The state of residual stresses across the composite may affect the structural integrity and load-bearing capacity of L-bend laminates. Thus, it is important to know the residual stress profile across its thickness. A better understanding of the stress distribution and failure mechanism of curved structures subjected to flexural load is significant. [1-8]

Lekhnitskii [9] developed basic equations of elasticity for stresses in an anisotropic cylindrical curved beam subjected to pure bending and Kedward et al [10] presented simple expressions for critical stress for delamination in curved laminates. Furthermore, Chang and Springer [11] numerically studied the effects of geometric parameters on the failure of L-bend composite laminates under critical loads. Additionally, the in-plane failure was determined using the Tsai-Hill criterion and also quadratic stress criterion was established to predict the out-of-plane failure. Sun and Kelly [12] studied the failure modes in L-shaped composite laminates with three different lamina arrangements. From the results, it is reported that failure is due to the interaction between delamination and transverse matrix cracking. Hiel et. al. [13] experimentally investigated delamination of elliptical and semicircular curved beam samples subjected to static and fatigue loads. The critical load for semi-circular beam failure was found to be highly sensitive to known defects in laminates. A catastrophic failure in laminates cured under room temperature subjected to both static and fatigue loads was observed. Avalon and Donaldson [14] investigated the effect of geometrical parameters (Curvature radius, thickness) on curved composite laminate and nano-additive on critical stress for the delamination, but the critical stress was found to be independent of nano-additives and geometrical parameters. Similar investigations by Hao et al. [15] found that the CBS increased with an increase in thickness of composite laminate and the effect of thickness variation on critical stress for failure is higher than that of radius to thickness ratio. Critical strain release rates were found to be very low during the inception of delamination and its subsequent



propagation in  $0^\circ/0^\circ$  fiber interface. Most et al. [16] compared the interlaminar stresses predicted in curved laminates by the analytical techniques with those obtained from finite element (FE) simulation. FE simulations predicted stresses were more accurate compared to the analytical methods, but computation costs are very high, hence it is necessary to develop new models that can compute the stresses closer to actual values at a lower cost. Cao et. al [17] carried an FE simulation to investigate the multifaceted failure of curved composite laminates and validated the results with the experimental findings. The 3D simulation with cohesive elements to predict the stress distribution in curved laminates included the interlaminar delamination, intralaminar matrix cracking and interaction between delamination and matrix cracking considering the free edge effect. Ranz et. al [18] used the improved Cohesive Zone Model (CZM) to predict the delamination in the curved laminate by incorporating the fiber bridging and the element size variation across its thickness of the curved region. The results of improved CZM were closer to the experimental findings compared to conventional CZM. In a recent study, Cinara et al [19] studied the effects of residual stresses on the failure mechanism of L-bend composite under pure bending using FE simulation. Numerical analysis of L-bend was carried with and without considering residual stresses. Residual stresses were found to be small to change the curved region and did not any effect on the initial failure mode. Yavuz et al [20] investigated the effect of lamina interface on interlaminar strength of CE curved laminate and concluded that laminate with  $0^\circ/0^\circ$  interfaces exhibits higher strength than composite with  $+45^\circ/-45^\circ$  interface.

Although many works have been carried to investigate the bending strength of curved laminates, limited work was observed in the literature, which was on the effects of residual stresses on bending strength of L-bend laminates. Hence, this work aims to conduct experimental investigations to determine the residual stresses in curved laminates and to study their effects on the failure of L-bend composite laminates. GE laminates with two different thicknesses were manufactured and post-cured at three different temperatures. The stresses induced after the processing of composite laminates were determined experimentally by employing Slitting method. The interlaminar radial stress for delamination of L-bend laminates were determined experimentally using a four-point bending test. Additionally, Fractographic examination of the delaminated surfaces were carried using SEM to know failure mechanisms due to delamination, fiber-matrix adhesion and matrix deformation at the interface etc.

## EXPERIMENTATIONS

### *Materials and manufacturing*

Unidirectional (UD) Glass fibers were used as reinforcements and Epoxy (LY 556) cured by 10 wt. % of Hardener (HY 951) as matrix. L-bend GE laminates  $[0]_{12}$  and  $[0]_{16}$  were prepared by the Hand layup method using two inverted V-shaped molds and cured at room temperature (RT). The bottom inverted V-shaped mold is shown in Fig. 1(a). L-bend laminates for determination of bending strength were cut as per ASTM D 6415 [21], which is shown in Fig. 1(b). Composite laminates were then post-cured using different curing temperatures.

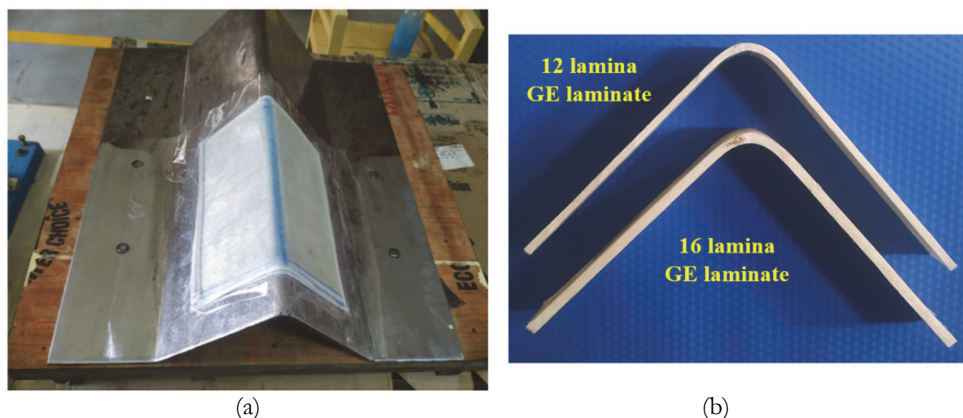


Figure 1. (a) Inverted bottom V-shaped mold for L-bend fabrication and (b) 16 and 12 lamina GE laminates.

### *Post-curing of laminates*

The state of residual stresses in curved laminates were varied by post-curing at different temperatures ( $90^\circ\text{C}$ ,  $135^\circ\text{C}$  and  $180^\circ\text{C}$ ) for about 6 hours and then cooled to RT with a cooling rate of  $-20^\circ\text{C}/\text{min}$ . The post-cured L-bend GE laminates are coded based on lamina sequence and post-curing conditions, which are given in Tab. 1.

Stacking of Lamina	Details of post-curing	GE laminates
	Cured under RT	GE-RT-12L
[0] <sub>12</sub>	Laminates were held at 90°C for 6 hours and cooled to RT with a cooling rate of 20°C /min.	GE-90-12L
	Laminates were held at 135°C for 6 hours and cooled to RT with a cooling rate of 20°C /min.	GE-135-12L
	Laminates were held at 180°C for 6 hours and cooled to RT with a cooling rate of 20°C /min.	GE-180-12L
	Cured under RT	GE-RT-16L
[0] <sub>16</sub>	Laminates were held at 90°C for 6 hours and cooled to RT with a cooling rate of 20°C /min.	GE-90-16L
	Laminates were held at 135°C for 6 hours and cooled to RT with a cooling rate of 20°C /min.	GE-135-16L
	Laminates were held at 180°C for 6 hours and cooled to RT with a cooling rate of 20°C /min.	GE-180-16L

Table 1: L-bend composite laminate codes based on laminas and post-curing condition

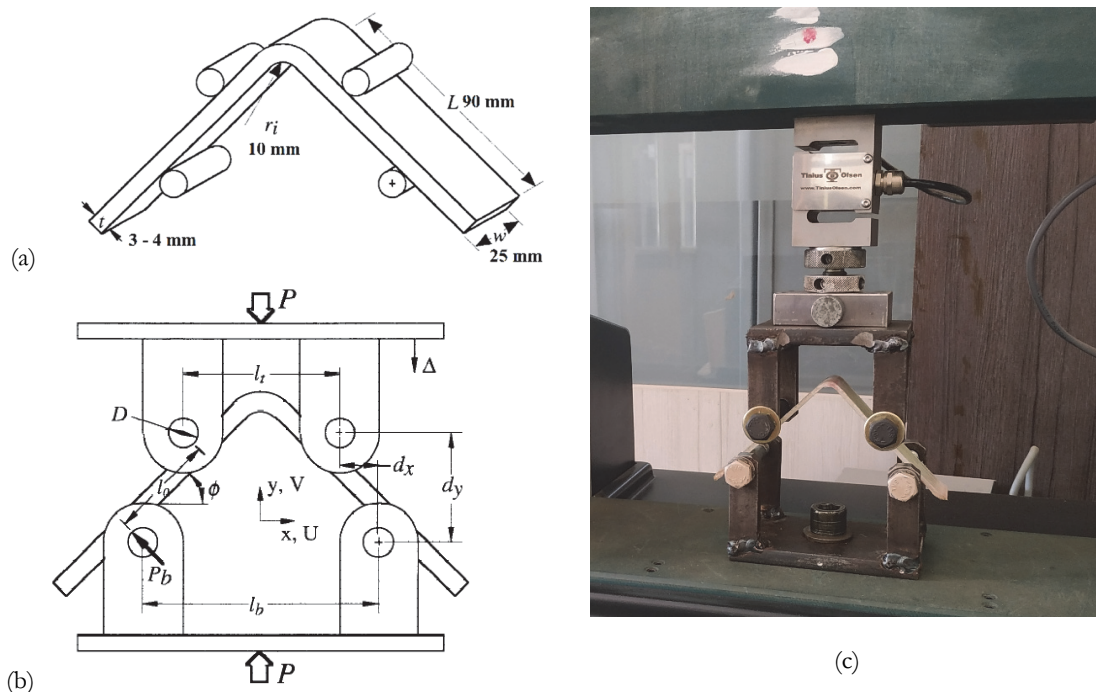


Figure 2: (a) Dimensions of L-bend composite (b) Four point bending fixture and (c) Manufactured four-point bending fixture for testing of L-bend composite.

## EXPERIMENTAL TECHNIQUES

### Four-point bending test

The critical stress for the delamination of L-bend composite laminates were evaluated by employing a four-point bending test as per ASTM D 6415. The geometric dimensions of curved GE laminates are shown in Fig. 2(a). The L-bend laminates were loaded under pure bending using a four-point bending fixture as shown in Fig. 2(b). The four-point bending fixture used in this work for testing is shown in Fig. 2(c). The rollers in the fixture have a diameter ( $D$ ) of 10 mm. The laminates were placed on two bottom rollers with a distance between them being 75 mm ( $l_b$ ). A gradual load



was applied to curved laminates through the top rollers placed at a distance of 50 mm ( $l_t$ ) from each other. The tests were carried out using Tinius Olsen UTM of 10kN capacity with a crosshead velocity of 1 mm/min. Five specimens from each configuration were tested and average value was used to obtain the critical stress.

Curved Beam Strength (CBS) indicates the minimum bending moment per unit width required to initiate the delamination in curved laminates. CBS is determined using Eqn. (1) and the load which causes the inception of delamination in curved laminates is used for calculations. The equation for interlaminar radial stress under pure bending was developed by Lekhnitskii [9] and is calculated using Eqns. (2) - (6)

$$CBS = \frac{M}{w} = \left( \frac{P}{2w \cos \theta} \right) \left( \left( \frac{d_x}{\cos \theta} \right) + (D + t) \tan \theta \right) \quad (1)$$

$$\sigma_r = - \left( \frac{CBS}{r_0^2 g} \right) \left[ 1 - \frac{(1 - \rho^{k+1})}{(1 - \rho^{2k})} \left( \frac{r_m}{r_0} \right)^{k-1} - \frac{(1 - \rho^{k-1})}{(1 - \rho^{2k})} \rho^{k+1} \left( \frac{r_0}{r_m} \right)^{k+1} \right] \quad (2)$$

where,

$$\rho = \frac{r_i}{r_0} \quad (3)$$

$$k = \sqrt{\frac{E_\theta}{E_r}} \quad (4)$$

$$g = \frac{1 - \rho^2}{2} - \frac{k}{k+1} \frac{(1 - \rho^{k+1})^2}{1 - \rho^{2k}} + \frac{k\rho^2}{k-1} \frac{(1 - \rho^{k-1})^2}{1 - \rho^{2k}} \quad (5)$$

$$r_m = \left[ \frac{(1 - \rho^{k-1})(k+1)(\rho r_o)^{k+1}}{(1 - \rho^{k+1})(k-1)(r_o)^{-(k-1)}} \right]^{\frac{1}{2k}} \quad (6)$$

where 'M' is bending moment; 'w' and 't' are the width and thickness of specimen respectively; 'P' is the load applied; 'dx' and 'dy' are horizontal and vertical distances between rollers on either side of bending fixture respectively; ' $\theta$ ' is the angle between specimen leg and horizontal reference line; 'ri' and 'ro' are the inner and outer radii of curved portion in L-bend laminates; 'rm' is a radial position of the maximum interlaminar (radial) tensile stress; 'g', 'k', 'g' are the parameters used in strength calculations and ' $\sigma_r$ ' is the radial stress in curved section; ' $E_\theta$ ' and ' $E_r$ ' are the elastic moduli in the radial and tangential direction respectively.

## RESIDUAL STRESS DETERMINATION USING THE SLITTING METHOD

The slitting method [22-32] is one of the most commonly employed semi destructive method for the characterization of residual stress profile in composite laminates. In this method an incremental cut was made to generate a thin slit across the stressed specimen and the strains relaxed due to each incremental cut are measured by a bonded strain gage as shown in Fig. 3.

A slit is machined in incremental cuts along with its thickness in the X-direction and the corresponding relaxed strains due to each incremental machining are measured using a bonded strain gage as shown in Fig. 3. The measured strains are utilized to determine the residual stresses in each lamina of the composite laminate. This method can determine residual stresses in only one direction (perpendicular to the direction incremental slit i.e. along Y-direction).

The relaxation of residual stresses occurs at one region and strains measured due to the corresponding relaxation are in the corresponding portion. So the equations relating the unknown residual stresses and the recorded strains are not in a simple form but have an integral form given by Eqn. (7).

$$\varepsilon_{yy}(a_i) = \int_0^{a_i} C(x, a_i) \sigma_{yy}(x) dx \quad (7)$$

where  $\varepsilon_{yy}(a_i)$  are the recorded strains when the incremental depth of cut is  $a_i$ ,  $\sigma_{yy}$  are the residual stresses to be determined and  $C(x, a_i)$  is kernel function which is equal to strains measured when unit stress is applied at depth 'x' within a slit of depth ' $a_i$ ' and needs to be obtained by FE analysis.

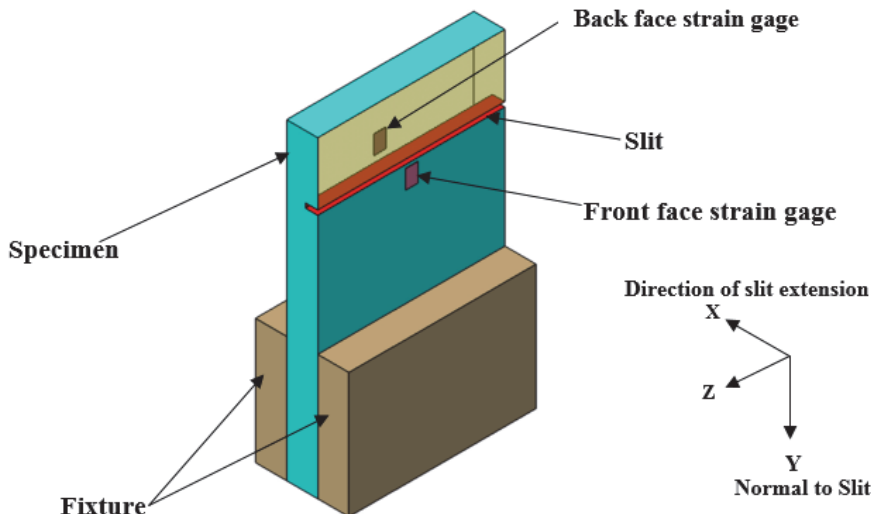


Figure 3: Slitting of the composite specimen.

To solve Eqn. (7), it is necessary to assume the initial profile of the residual stresses which are to be determined. This profile defines how the stresses vary within the lamina or the entire composite.

In fiber-reinforced laminated composites, as there is a discontinuity in material properties across the lamina borders, the stress profile is not continuous. For such types of materials where the material properties vary along with the thickness, the stress profile is approximated by a technique known as the Pulse method. The main benefit of this approximation is that it does not require the condition of continuity of the residual stress profile and thus can be applied for laminated composites. In this method of approximation, residual stresses are presumed to be constant over each depth of cut and given by Eqn. (8).

$$\sigma(x_j) = \sum_{j=1}^n \sigma_j U_j(x) \quad (8)$$

where ' $\sigma_j$ ' denotes the stresses in the ' $j^{\text{th}}$ ' depth of cut when the 'total number of cuts' is ' $n$ '.

The pulse functions [ $U_j(x)$ ] can be given by Eqn. (9)

$$U_j(x) = \begin{cases} 1 & a_{j-1} \leq x \leq a_j \\ 0 & x < a_{j-1}, x > a_j \end{cases} \quad (9)$$

The unknown residual stresses and the measured strains for every depth of cut can be expressed in matrix form as

$$[C]\{\sigma\} = \{\varepsilon\} \quad (10)$$

where  $[C]$  is Compliance matrix,  $\{\sigma\}$  is Residual stress vector and  $\{\varepsilon\}$  – Recorded strain vector

The compliance matrix can be obtained by simulating each incremental cut of the slitting method using FE analysis. Each element of compliance matrix ' $C_{ij}$ ' corresponds to the strains measured across the strain gage when applied residual stresses are equal to unit load.



## COMPLIANCE COEFFICIENT MATRIX

**C**ompliance coefficient matrix is obtained by simulating each incremental depth of cut using FE analysis. The simulation is carried out with boundary conditions similar to the experimental slitting method, one end is fixed and an incremental slit is cut on the other end. The analysis is carried out using PLANE182 2D elements in ANSYS by applying the experimentally determined elastic constants (The elastic constants of GE laminates post-cured at different temperatures are provided as a supplementary file.).

The simulation of each incremental cut compromises two steps; the first step is to remove the elements from the slit area followed by an application of unit load across the slit, the resulting strains are averaged across the gauge location. Compliance matrices for different GE laminates are determined using their corresponding geometrical and material properties, these matrices are used to determine the residual stresses by using the corresponding measured relaxed strains. Totally eight compliance matrices were obtained by simulating the different GE laminates.

## SLITTING SPECIMEN PREPARATION

**T**he dimensions of the specimen used for the slitting experiment are given in Tab. 2. The slitting sample is carefully washed with acetone to remove any foreign particles and is prepared for strain gage bonding. A gauge of 1 mm gauge length is bonded on the sample at a distance of 15 mm from the top end which is shown in Fig. 4 (d).

Length in mm	Width in mm	Thickness in mm
75	20	3.0 – 4.0

Table 2: Dimensions of slitting specimen

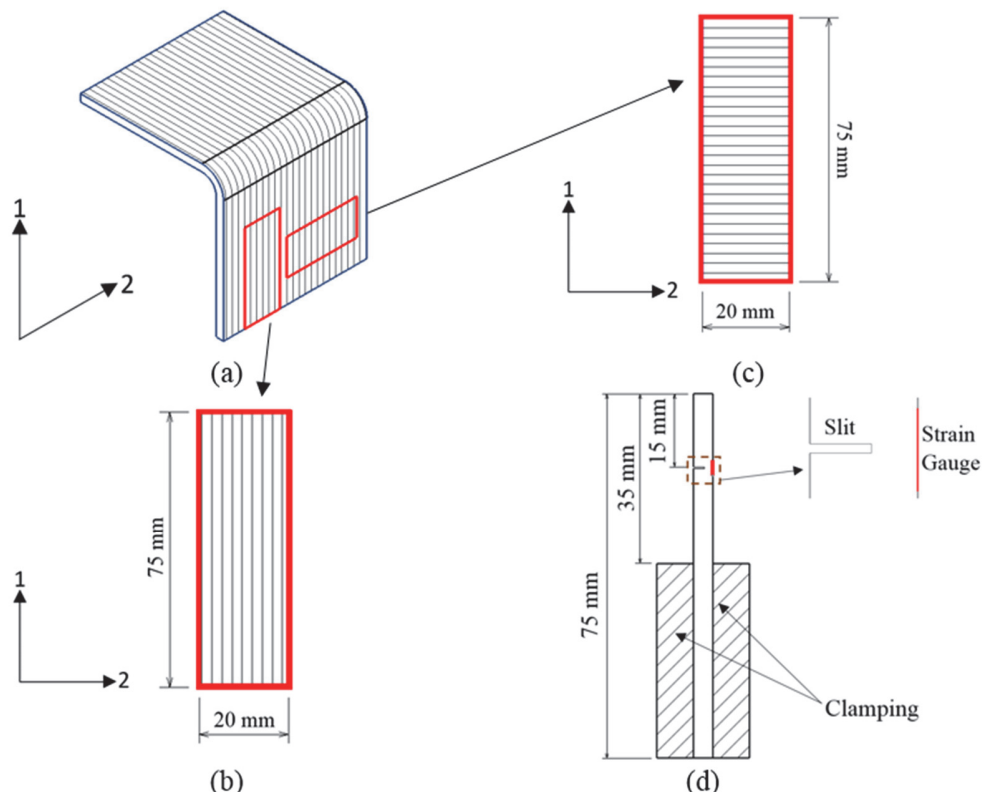


Figure 4: (a) L-bend composite laminate (b) Slitting Specimen used for determination of longitudinal residual stress. (c) Slitting Specimen used for determination of transverse residual stress. (d) Slitting specimen bonded with a strain gauge.

## RESULTS AND DISCUSSIONS

### *Process-induced residual stresses*

The relaxed (measured) strains versus slit depth of RT and post cured GE laminates in Longitudinal and Transverse directions were recorded and plotted in Fig.5. The residual stresses were calculated using the Pulse method from the measured strains. The profile of the cure induced stresses in the composite laminates depends on the temperature profile; the level and time period of the applied temperature and the cooling rate. The CTE of polymer matrix material is substantially higher than the fibers. CTE of fibers are usually orthotropic. CTE of fibers along fiber direction is low or negative, but higher along transverse direction. This leads to residual stresses during cool down even in unidirectional material. Higher the post curing temperature, higher the cure induced stresses in composite laminates. The results for unidirectional samples demonstrated that strains were only significant in the longitudinal direction and is extremely small in the other two directions [26, 32-33]. It was observed from the measured strains plot that the strains in all GE laminates gradually increase with an increase in slit depth. The laminates post-cured at 180°C released higher strains compared to other GE laminates. From Fig. 5(a), it can be seen that the recorded strains in the first ply were tensile, as the stresses are compressive (Fig. 6(a)) across the transverse direction, the stresses are compressive on the outer layers and both tensile/compressive at the inner layers (Fig. 6(a)). In a UD lamina a longitudinal tensile stress develops in the matrix which must then be balanced by an equal and opposite compressive stress in the reinforcing fibers. From Fig. 5(b), it can be observed that the measured strains in the first ply are compressive, as the stresses are tensile and compressive on the outer layers (Fig. 6(b)) and similar trends can be observed in the 6(c) and 6(d).

The longitudinal and transverse residual stresses of GE laminates are plotted in Fig. 6. Longitudinal residual stresses in GE laminates with 12 and 16 laminas varied between -8.59 MPa to +7.83 MPa and -10.47 MPa to +11.06 MPa respectively. Whereas, the transverse residual stresses in GE laminates with 12 and 16 laminas varied between -7.56 MPa to +6.45 MPa and -2.78 MPa to + 5.91 MPa respectively.

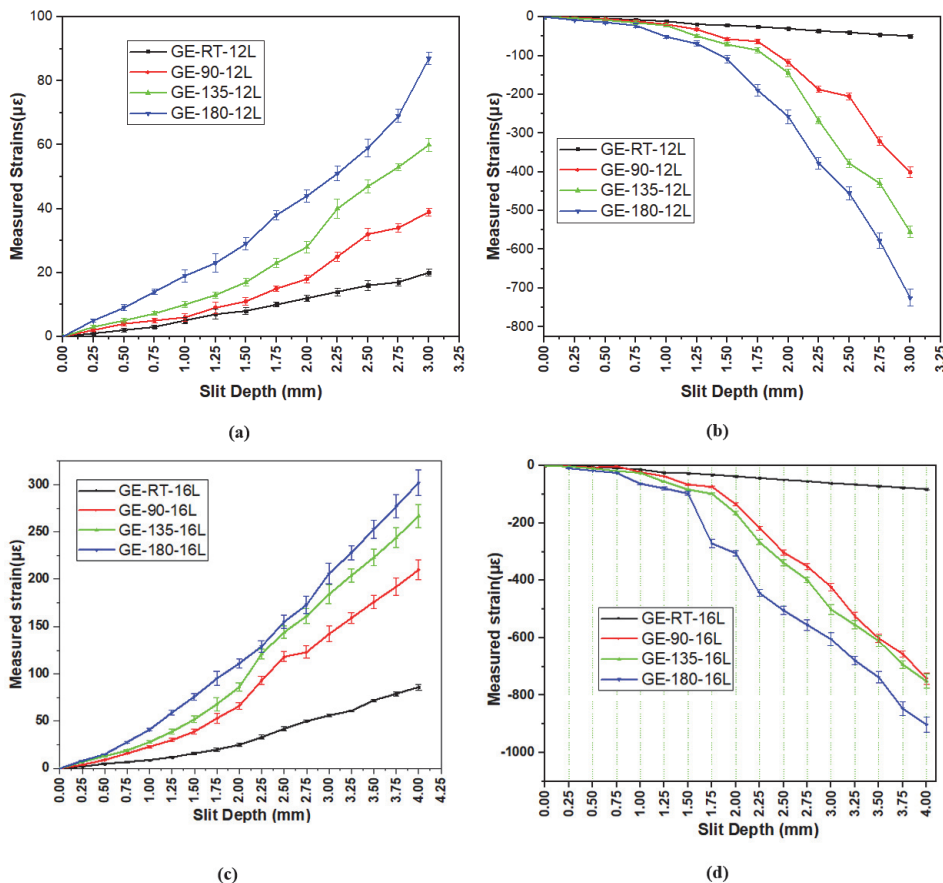


Figure 5: Plots showing measured or relaxed strains versus incremental slit depth of various GE laminates. (a) and (b) transverse and Longitudinal Strains in GE laminates with 12 laminas. (c) and (d) transverse and Longitudinal Strains in GE laminates with 16 laminas.

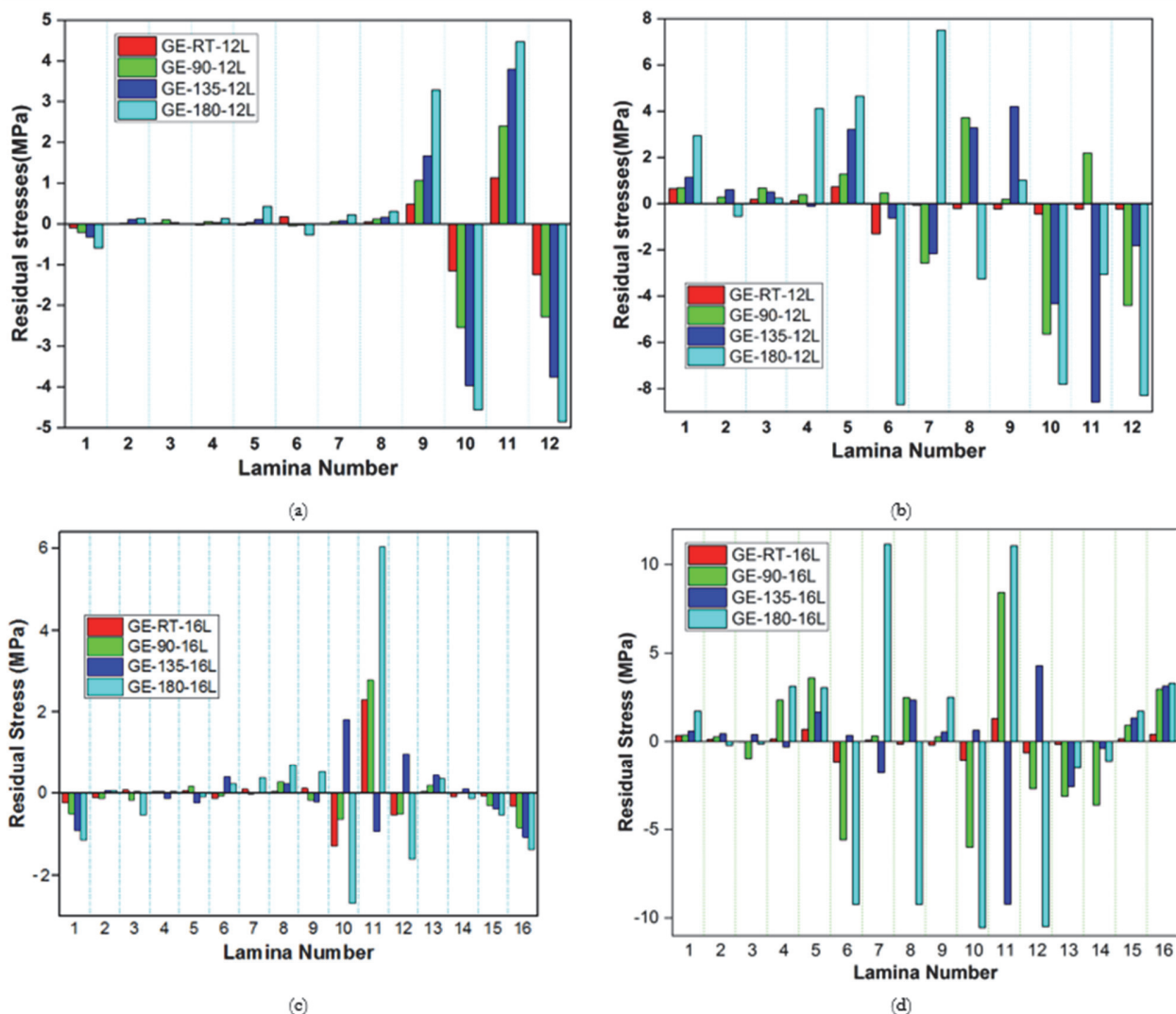


Figure 6: Bar charts showing Residual stresses versus lamina number of all the GE laminates. (a) and (b) transverse and longitudinal residual stress in each lamina of 12 laminas GE laminate. (c) and (d) Transverse and longitudinal residual stress in each lamina of 16 laminas GE laminate.

#### *CBS and interlaminar radial stress*

The graphs depicting the applied load with the loading jaw displacements obtained from the four-point bending test of GE laminates are shown in Fig. 7. It was observed that all the GE laminates tend to bend elastically till the load reaches maximum values. This nature of bending depends on the thickness of GE laminates and post-curing temperature. Furthermore, it was seen that there is a sudden drop in the bending load, indicating the inception of the delamination in GE laminates. The slope of the load-displacement curve depends on the thickness and post-curing temperature of GE laminates. GE laminates with 16 laminas showed higher stiffness than laminates made up of 12 Laminas. CBS and calculated interlaminar radial stress of all GE laminates are shown in Fig.8 and Fig. 9 respectively. The maximum load required for initiation of delamination depends on the thickness of L-bend laminates and post-curing temperature. GE laminates post-cured at 180 °C (GE-180-12L and GE-180-16L) required higher loads for delamination within their thickness groups as compared to laminates cured other than 180 °C. CBS of GE laminates increased with post-curing temperature and the laminates cured at 180 °C (GE-180-12L and GE-180-16L) exhibited higher CBS as compared to other post cured laminates. From Fig. 9, interlaminar radial stress in GE laminates increased with post-curing temperature and is independent of the laminate thickness. GE laminates with 12 and 16 laminas post-cured at the same temperature exhibited almost similar critical stress. GE laminates post-cured at 180 °C (GE-180-12L and GE-180-16L) have critical stress around 74 MPa for initial delamination and this is higher when compared to other GE laminates.

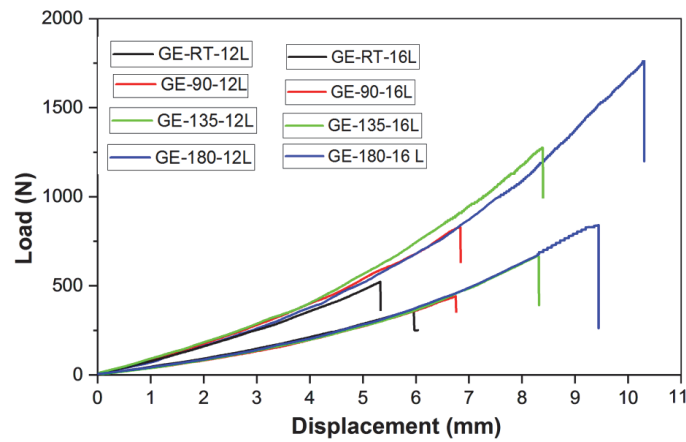


Figure 7: Load–displacement response of L-bend GE composite laminates under four-point bending load.

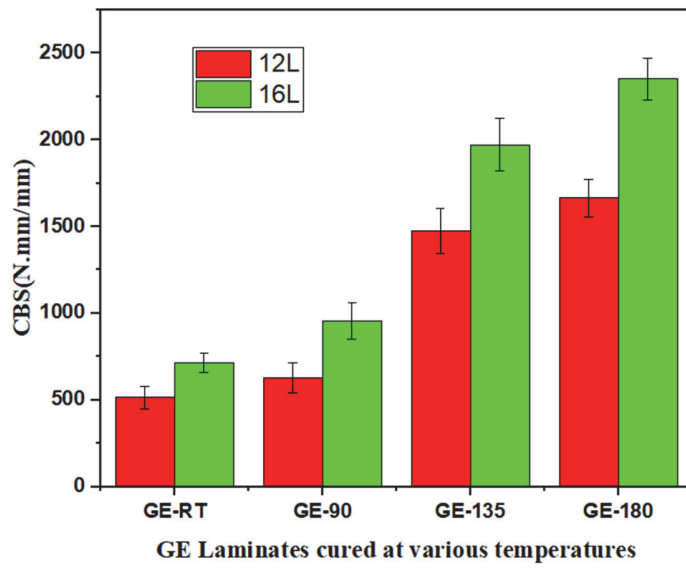


Figure 8: CBS of the all GE composite laminates.

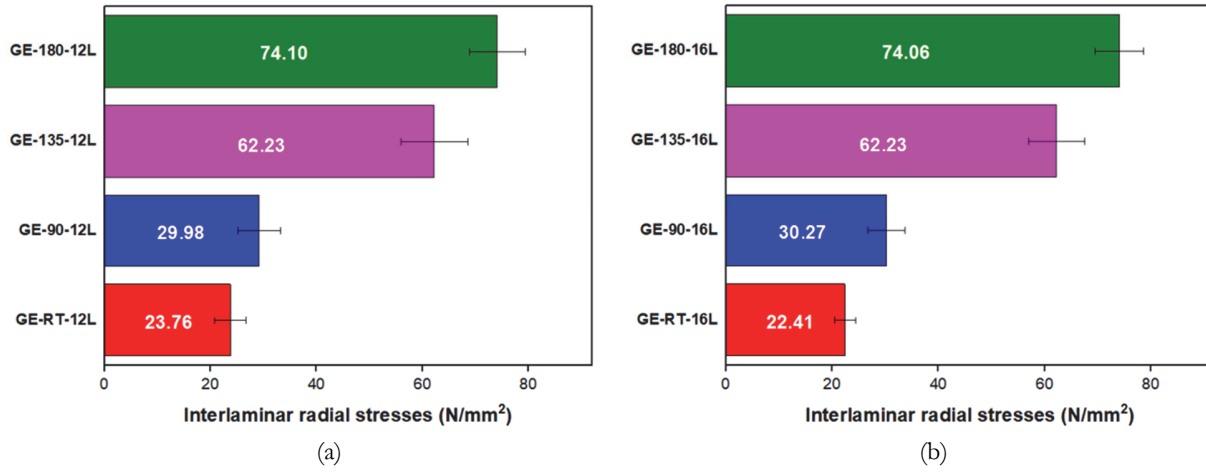


Figure 9: Interlaminar radial stresses in GE laminates with (a) 12 Laminas and (b) 16 Laminas.



### Effects of residual stresses on interlaminar radial stress

The critical stress for initial delamination in GE laminates with 12 and 16 laminas post-cured at the same temperature are almost the same, hence it can be claimed that the state of residual stresses does not have a noticeable effect on the critical stresses. The residual stresses in composite laminates do not change the region of curvature (The angle between the legs of L-bend remains unchanged after post-curing), so the critical stress for delamination is not affected by the state of residual stress in the L-bend composite laminates. The residual stresses formed during the processing were within 12 MPa and are very small to effect the bending strength of L-bend laminates.

The initial delamination of GE laminates under the bending load was observed to occur almost across 50 % of the thickness. The location of delamination in GE laminates with reference from the bottom lamina is given in Tab. 3.

GE laminate	Location of delamination with reference from bottom lamina in % of the total thickness	GE laminate	Location of delamination with reference from bottom lamina in % of the total thickness
GE-RT-12L	58.64 %	GE-RT-16L	49.31 %
GE-90-12L	51.64 %	GE-90-16L	47.25 %
GE-135-12L	55.55 %	GE-135-16L	51.33 %
GE-180-12L	53.27 %	GE-180-16L	46.28 %

Table 3: Location of delamination in GE laminates with reference from the bottom lamina.

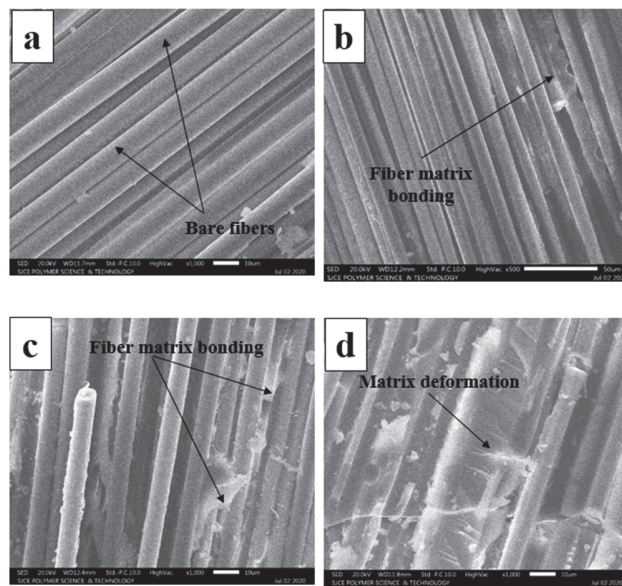


Figure 10: SEM images from delaminated surfaces of (a) GE-RT-16L (b) GE-90-16L, (c) GE-135-16L (d) GE-180-16L.

### SCANNING ELECTRON MICROSCOPIC (SEM) ANALYSIS

To understand the post-curing effects on delamination of curved laminates, the delaminated surfaces of post-cured GE laminates with 16 laminas were studied using SEM. The morphology of delaminated surfaces was characterized using the JEOL JSM-IT300 machine. SEM images from delaminates surfaces of GE laminates with 16 plies are shown in Fig. 10. The micrographs were characterized based on matrix deformation, fiber-matrix interfacial bonding and fiber bridging phenomenon. [34-35].

From Fig. 10(a), for GE-RT-16L the fibers are bare and are plainly visible without any noticeable matrix adhesion implying a weak interfacial bonding of fiber and matrix. A fiber-matrix adhesion can be observed in Fig. 10(b), indicating a good interface bonding in GE-90-16L laminate. From the micrographs of post-cured GE laminates, GE-180-16L exhibits matrix deformation and good fiber-matrix bonding indicating a better resistance to delamination compared to GE-135-16L and other composite laminates. As the curing temperature increased, the GE laminates exhibited a good fiber-matrix bonding



and a higher resistance to delamination is observed. A strong fiber-matrix interfacial bond in GE-180-12L composite is further appreciated by higher delamination resistance, CBS and critical stress compared to other post cured composites.

## CONCLUSIONS

The effects of residual stresses on interlaminar radial stress in GE L-bend laminates were experimentally investigated. GE laminates with 12 and 16 laminas were manufactured using two inverted V-shaped molds by hand lamination technique. The state of residual stresses in GE laminates was varied by post-curing the GE laminates using different curing temperatures. The process-induced stress profile in each GE laminate was characterized by employing the slitting method. The critical stress required for initial delamination in all L-bend GE laminates was experimentally determined using four points bending fixture as per ASTM D6415. The following conclusions can be drawn from this work.

The slope of the load-displacement curve depends on the thickness of the GE laminates and is almost independent of the curing temperature, whereas the CBS and maximum load required for initiation of delamination depend on both thickness and post-curing temperature.

Longitudinal residual stresses in GE laminates with 12 and 16 laminas varied between -8.59 MPa to +7.83 MPa and -10.47 MPa to +11.06 MPa respectively. Whereas, the transverse residual stresses in GE laminates with 12 and 16 laminas varied between -7.56 MPa to +6.45 MPa and -2.78 MPa to + 5.91 MPa respectively.

Interlaminar radial stress in GE laminates increased with post-curing temperature and is independent of the thickness of the laminates. The critical stress for initial delamination in GE laminates with 12 and 16 laminas post-cured at the same temperature is almost the same and so it can be claimed that the state of residual stresses does not have a noticeable effect on the critical stresses. The initial delamination of GE laminates under the bending load was observed to occur almost across 50 % of the thickness.

From the SEM micrographs, it was observed that the increase in the critical stress for delamination with an increase in post-curing temperature can be attributed to the temperature-dependent matrix deformation. The increase in critical stress may be due to improved bonding between fiber-matrix interfaces after curing at a higher temperature.

## CONFLICT OF INTEREST

The authors declare that there is no conflict of interest.

T

## ACKNOWLEDGMENTS

The authors would like to acknowledge the Directorate of Minorities, Government of Karnataka (GOKDOM), Bengaluru.

The authors thankfully acknowledge the funding and support provided by the Deanship of Scientific Research, King Khalid University, Abha-Asir, Kingdom of Saudi Arabia, with grant number R.G.P.2/6/38 under research group-Materials and Production, to complete the research work.

The authors of this paper appraise their appreciation to the organization for providing required facilities at Research Center Mechanical engineering department of SDM College of Engineering and Technology, Dharwad for their motivation and backing throughout the investigation. The authors would like to acknowledge the Center for Material Science, School of Mechanical Engineering, KLE Technological University, Hubballi, Karnataka, India

## REFERENCES

- [1] Shivakumar Gouda, P.S., Vijay, C. and Barhai, P. K. (2017) Fracture toughness of glass epoxy laminates using carbon nano particles and ETBN rubber. Mater Perform Characterization 6(1), pp. 488–499. DOI: 10.1520/MPC20170027.



- [2] Withers, P.J. and Bhadeshia, H.K.D.H. (2001). Residual stress. Part 2—Nature and origins. *Materials science and technology*, 17(4), pp. 366-375. DOI:10.1179/026708301101510087.
- [3] Ranz, D., Cuartero, J., Miravete, A. and Miralbes, R. (2017). Experimental research into interlaminar tensile strength of carbon/epoxy laminated curved beams. *Composite Structures*, 164, pp.189-197. DOI: 10.1016/j.compstruct.2016.12.010.
- [4] Gumgol, U., Umarfarooq, M.A., Huddar, D., Vastrad, J.V., Wilkinson, A. and Shivakumar Gouda, P.S. (2019). Influence of Kenaf and GO on interlaminar radial stresses in glass/epoxy L-bend laminates. *SN Applied Sciences*, 1(1), pp.1-8. DOI:10.1007/s42452-018-0108-6.
- [5] Takagaki, K., Minakuchi, S. and Takeda, N. (2017). Process-induced strain and distortion in curved composites. Part II: Parametric study and application. *Composites Part A: Applied Science and Manufacturing*, 103, pp.219-229. DOI: 10.1016/j.compositesa.2017.09.019
- [6] Werner, B.T., Nelson, S.M. and Briggs, T.M. (2018). Effect of process induced stresses on measurement of frp strain energy release rates. *Mechanics of Composite and Multi-functional Materials*, Springer, Cham, 6, pp. 157-174. DOI: 10.1007/978-3-319-63408-1\_16
- [7] Shokrieh, M.M. and Kamali, S.M. (2005). Theoretical and experimental studies on residual stresses in laminated polymer composites. *Journal of composite materials*, 39(24), pp.2213-2225. DOI: 10.1177/0021998305053511
- [8] Brunner, A.J., (2020). Fracture mechanics of polymer composites in aerospace applications. In *Polymer composites in the aerospace industry*, pp. 195-252. Woodhead Publishing. DOI: 10.1016/B978-0-85709-523-7.00008-6
- [9] Lekhnitskii, S.G., (1968). Chapter IX. Theory of Bending of Anisotropic Plates (thin plates). *Anisotropic Plates*, Gordon and Breach, Science Publishers, New York, USA, pp.533.
- [10] Kedward, K.T., Wilson, R.S. and McLean, S.K. (1989). Flexure of simply curved composite shapes. *Composites*, 20(6), pp.527-536. DOI: 10.1016/0010-4361(89)90911-7.
- [11] Chang, F.K. and Springer, G.S. (1986). The strengths of fiber reinforced composite bends. *Journal of composite materials*, 20(1), pp. 30-45. DOI: 10.1177/002199838602000103.
- [12] Sun, C.T. and Kelly, S.R. (1988). Failure in composite angle structures part I: Initial failure. *Journal of reinforced plastics and composites*, 7(3), pp. 220-232. DOI: 10.1177/073168448800700302.
- [13] Hiel, C.C., Sumich, M. and Chappell, D.P. (1991). A curved beam test specimen for determining the interlaminar tensile strength of a laminated composite. *Journal of Composite Materials*, 25(7), pp. 854-868. DOI: 10.1177/002199839102500705.
- [14] Avalon, S.C. and Donaldson, S.L. (2011). Strength of composite angle brackets with multiple geometries and nanofiber-enhanced resins. *Journal of composite materials*, 45(9), pp. 1017-1030. DOI: 10.1177/0021998310381538.
- [15] Hao, W., Ge, D., Ma, Y., Yao, X. and Shi, Y. (2012). Experimental investigation on deformation and strength of carbon/epoxy laminated curved beams. *Polymer Testing*, 31(4), pp. 520-526. DOI: 10.1016/j.polymertesting.2012.02.003.
- [16] Most, J., Stegmair, D. and Petry, D. (2015). Error estimation between simple, closed-form analytical formulae and full-scale FEM for interlaminar stress prediction in curved laminates. *Composite Structures*, 131, pp. 72-81. DOI: 10.1016/j.compstruct.2015.03.075
- [17] Cao, D., Hu, H., Duan, Q., Song, P. and Li, S. (2019). Experimental and three-dimensional numerical investigation of matrix cracking and delamination interaction with edge effect of curved composite laminates. *Composite Structures*, 225, pp.111154. DOI: 10.1016/j.compstruct.2021.113963
- [18] Ranz, D., Cuartero, J., Castejón, L., Miralbes, R. and Valladares, D. (2020). Enhanced cohesive zone model to predict delamination behavior of carbon/epoxy laminated curved beams. *Mechanics of Advanced Materials and Structures*, pp. 1-11. DOI: 10.1080/15376494.2020.1769232
- [19] Cinar, K., Guven, I. and Ersoy, N. (2020). Effect of residual stress on the bending response of L-shaped composite laminates. *Composite Structures*, 246, pp.112425. DOI: 10.1016/j.compstruct.2020.112425
- [20] Yavuz, B.O., Parnas, L. and Coker, D. (2019). Interlaminar tensile strength of different angle-ply CFRP composites. *Procedia Structural Integrity*, 21, pp. 198-205. DOI: 10.1016/j.prostr.2019.12.102
- [21] ASTM D6415 / D6415M-06a. (2013), Standard Test Method for Measuring the Curved Beam Strength of a Fiber-Reinforced Polymer-Matrix Composite, ASTM International, West Conshohocken, PA, www.astm.org. DOI: 10.1520/D6415\_D6415M-06AR13
- [22] Shokrieh, M.M., Akbari, S. and Daneshvar, A. (2013). A comparison between the slitting method and the classical lamination theory in determination of macro-residual stresses in laminated composites. *Composite Structures*, 96, pp.708-715. DOI: 10.1016/j.compstruct.2012.10.001



- [23] Umarfarooq, M.A., Gouda, P.S., Banapurmath, N.R. and Edacherian, A. (2019). Impact of process induced residual stresses on interlaminar fracture toughness in carbon epoxy composites. *Composites Part A: Applied Science and Manufacturing*, 127, pp.105652. DOI: 10.1016/j.compositesa.2019.105652
- [24] Akbari, S., Taheri-Behrooz, F. and Shokrieh, M.M. (2013). Slitting measurement of residual hoop stresses through the wall-thickness of a filament wound composite ring. *Experimental Mechanics*, 53(9), pp.1509-1518. DOI: 10.1007/s11340-013-9768-8
- [25] Prime, M.B. (1999). Residual stress measurement by successive extension of a slot: the crack compliance method, 52(2), pp.75–96. DOI: 10.1115/1.3098926
- [26] Ghasemi, A.R. and Mohammadi, M.M. (2016). Residual stress measurement of fiber metal laminates using incremental hole-drilling technique in consideration of the integral method. *International Journal of Mechanical Sciences*, 114, pp. 246-256. DOI: 10.1016/j.ijmecsci.2016.05.025
- [27] Ghasemi, A.R., Tabatabaeian, A. and Asghari, B. (2019). Application of slitting method to characterize the effects of thermal fatigue, lay-up arrangement and MWCNTs on the residual stresses of laminated composites. *Mechanics of Materials*, 134, pp. 185-192. DOI: 10.1016/j.mechmat.2019.04.008
- [28] Schajer, G.S. and Prime, M.B. (2006). Use of inverse solutions for residual stress measurements. 128(3), pp. 375–382. DOI: 10.1115/1.2204952
- [29] Cheng, W. and Finnie, I. (2007). Residual stress measurement and the slitting method. Springer Science & Business Media.
- [30] Schajer, G.S. ed. (2013). Practical residual stress measurement methods. John Wiley & Sons.
- [31] Umarfarooq, M.A., Gouda, P.S., Nandibewoor, A., Banapurmath, N.R. and Kumar, G.V. (2019). Determination of residual stresses in GFRP composite using incremental slitting method by the aid of strain gauge. In AIP Conference Proceedings, AIP Publishing LLC. 2057(1), pp. 020038. DOI: 10.1063/1.5085609.
- [32] Mahmood M Shokrieh, ed. (2014). Residual stresses in composite materials. Woodhead publishing.
- [33] Wisnom, M.R., Gigliotti, M., Ersoy, N., Campbell, M. and Potter, K.D. (2006). Mechanisms generating residual stresses and distortion during manufacture of polymer–matrix composite structures. *Composites Part A: Applied Science and Manufacturing*, 37(4), pp. 522-529. DOI: 10.1016/j.compositesa.2005.05.019.
- [34] Hiley, M.J. (1999). Fractographic study of static and fatigue failures in polymer composites. *Plastics, rubber and composites*, 28(5), pp. 210-227. DOI: 10.1179/146580199101540358.
- [35] Franco, L.A. (2011). Fractography of composite materials. Wiley Encyclopedia of Composites, pp.1-16.
- [36] Kaw, A.K. (2005). Mechanics of composite materials. CRC press.